DISCRETE AND CONTINUOUS
DYNAMICAL SYSTEMS SERIES B
Volume **26**, Number **1**, January **2021**

doi:10.3934/dcdsb.2020351

pp. **61–79**

AN ADAPTIVE FINITE ELEMENT DTN METHOD FOR THE THREE-DIMENSIONAL ACOUSTIC SCATTERING PROBLEM

Gang Bao*, Mingming Zhang and Bin Hu

School of Mathematical Sciences, Zhejiang University
Hangzhou 310027, China

Peijun Li

Department of Mathematics, Purdue University
West Lafayette, IN 47907, USA

Abstract. This paper is concerned with a numerical solution of the acoustic scattering by a bounded impenetrable obstacle in three dimensions. The obstacle scattering problem is formulated as a boundary value problem in a bounded domain by using a Dirichlet-to-Neumann (DtN) operator. An a posteriori error estimate is derived for the finite element method with the truncated DtN operator. The a posteriori error estimate consists of the finite element approximation error and the truncation error of the DtN operator, where the latter is shown to decay exponentially with respect to the truncation parameter. Based on the a posteriori error estimate, an adaptive finite element method is developed for the obstacle scattering problem. The truncation parameter is determined by the truncation error of the DtN operator and the mesh elements for local refinement are marked through the finite element approximation error. Numerical experiments are presented to demonstrate the effectiveness of the proposed method.

1. **Introduction.** Wave scattering by bounded impenetrable media is usually referred to as the obstacle scattering problem. It has played an important role in many scientific areas such as radar and sonar, non-destructive testing, medical imaging, geophysical exploration, and nano-optics [2, 13]. Due to the significant applications, the obstacle scattering problem has been extensively studied in the past several decades. Consequently, a variety of methods have been developed to solve the scattering problem mathematically and numerically such as the method of boundary integral equations [12, 29] and the finite element method [24, 28]. This paper concerns a numerical solution of the acoustic wave scattering by an obstacle in three dimensions.

As an exterior boundary value problem, the obstacle scattering problem is formulated in an open domain, which needs to be truncated into a bounded computational domain when applying numerical methods such as the finite element method. It is indispensable to impose a boundary condition on the boundary of the truncated

2020 *Mathematics Subject Classification.* Primary: 65N30, 78A45, Secondary: 35Q60, 78M10.
Key words and phrases. Acoustic scattering problem, adaptive finite element method, transparent boundary condition, a posteriori error estimates.
The first author is supported in part by an NSFC Innovative Group Fund (No.11621101). The last author is supported in part by the NSF grant DMS-1912704.

* Corresponding author: Gang Bao.

domain. The ideal boundary condition is to completely avoid artificial wave reflection by mimicking the wave propagation as if the boundary did not exist [7]. Such a boundary condition is called an absorbing boundary condition [14], a nonreflecting boundary condition [17], or a transparent boundary condition (TBC) [18]. It still remains as an active research topic in computational wave propagation [19], especially for time-domain scattering problems [3]. Since Berenger proposed the perfectly matched layer (PML) technique for the time-domain Maxwell equations [8], the PML method has been extensively studied for various wave propagation problems [6, 11, 31]. As an effective approach for the domain truncation, the basic idea of the PML technique is to surround the domain of interest by a layer of finite thickness with specially designed artificial medium that would attenuate all the waves coming from inside of the domain. Combined with the PML technique, the a posteriori error estimate based adaptive finite element methods were developed for the diffraction grating problems [10, 5] and the obstacle scattering problems [9]. It was shown that the estimates consist of the finite element discretization error and the PML truncation error which has an exponential rate of convergence with respect to the PML parameters.

Recently, an alternative adaptive finite element method was developed for solving the two-dimensional acoustic obstacle scattering problem [23] and the open cavity scattering problem [33], where the PML was replaced by the TBC to truncate the open domain. Since the TBC is exact, it can be imposed on the boundary which could be put as close as possible to the obstacle. Hence it does not require an extra absorbing layer of artificial medium to enclose the domain of interest. Based on a nonlocal Dirichlet-to-Neumann (DtN) operator, the TBC is given as an infinite Fourier series. Practically, the series needs to be truncated into a sum of finitely many, say N, terms, where N is an appropriately chosen positive integer. In [23], an a posteriori error estimate was derived for the finite element discretization but it did not include the truncation error of the DtN operator. The complete a posteriori error estimate was obtained in [22]. The new estimate takes into account both the finite element discretization error and the DtN operator truncation error. It was shown that the truncation error decays exponentially with respect to the truncation parameter N. The adaptive finite element DtN method has also been applied to solve the diffraction grating problems [32] as well as the elastic wave equation in periodic structures [26]. The numerical results show that the adaptive finite element DtN method is competitive with the adaptive finite element PML method. We refer to [27] for a continuous interior penalty finite element method (CIP-FEM) for solving high frequency scattering problems with the truncated DtN boundary condition.

In this work, we extend the analysis in [22] to the three-dimensional obstacle scattering problem. It is worthy to mention that the extension is nontrivial since more complex spherical Hankel functions need to be considered and the computation is more challenging in three dimensions. Specifically, we consider the acoustic wave scattering by a sound hard obstacle. Based on a TBC, the exterior problem is formulated equivalently into a boundary value problem in a bounded domain for the three-dimensional Helmholtz equation. Using a duality argument, we derive the a posteriori error estimate which includes the finite element discretization error and the DtN operator truncation error. Moreover, we show that the truncation error has an exponential rate of convergence with respect to the truncation parameter N. The a posteriori estimate is used to design the adaptive finite element algorithm

to choose elements for refinements and to determine the truncation parameter N. In addition, we present a technique to deal with adaptive mesh refinements of the surface. Numerical experiments are included to demonstrate the effectiveness of the proposed method.

This paper is organized as follows. In Section 2, we introduce the model problem of the acoustic wave scattering by an obstacle in three dimensions. The variational formulation is given for the boundary value problem by using the DtN operator. In Section 3, we present the finite element approximation with the truncated DtN operator. Section 4 is devoted to the a posteriori error analysis by using a duality argument. In Section 5, we discuss the numerical implementation and the adaptive finite element DtN method, and present two numerical examples to demonstrate the effectiveness of the proposed method. The paper is concluded with some general remarks and directions for future work in Section 6.

2. **Problem formulation.** Consider a bounded sound-hard obstacle D with Lipschitz continuous boundary ∂D in $\mathbb{R}^3$. Denote by $B_r = \{x \in \mathbb{R}^3 : |x| < r\}$ the ball which is centered at the origin and has a radius r. Let R and R' be two positive constants such that $R > R' > 0$ and $\overline{D} \subset B_{R'} \subset B_R$. Denote $\Omega = B_R \backslash \overline{D}$. The obstacle scattering problem for acoustic waves can be modeled by the following exterior boundary value problem:

$$\begin{cases} \Delta u + \kappa^2 u = 0 & \text{in } \mathbb{R}^3 \setminus \overline{D}, \\ \partial_\nu u = -g & \text{on } \partial D, \\ \lim\limits_{r\to\infty} r(\partial_r u - \mathrm{i}\kappa u) = 0, & r = |x|, \end{cases} \tag{1}$$

where $\kappa > 0$ is the wavenumber and ν is the unit outward normal vector to ∂D. Although the results are given for the sound-hard boundary condition in this paper, the method can be applied to other types of boundary conditions, such as the sound-soft and impedance boundary conditions.

Let $\hat{x}_1 = \sin\theta\cos\varphi$, $\hat{x}_2 = \sin\theta\sin\varphi$, $\hat{x}_3 = \cos\theta$, $\theta \in [0, \pi]$ and $\varphi \in [0, 2\pi]$. Introduce the spherical harmonic functions

$$Y_n^m(\hat{x}) = Y_n^m(\theta, \varphi) = \sqrt{\frac{(2n+1)(n-|m|)!}{4\pi(n+|m|)!}} P_n^{|m|}(\cos\theta) e^{\mathrm{i}m\varphi},$$

where $m = -n, \ldots, n$, $n = 0, 1, \ldots$, and

$$P_n^m(t) = (1-t^2)^{\frac{m}{2}} \frac{\mathrm{d}^m}{\mathrm{d}t^m} P_n(t), \quad -1 \le t \le 1,$$

are called the associated Legendre functions and P_n are the Legendre polynomials. It is known that the spherical harmonic functions $\{Y_n^m : m = -n, \ldots, n, n = 0, 1, \ldots\}$ form an orthonormal system in $L^2(\mathbb{S}^2)$, where $\mathbb{S}^2 = \{x \in \mathbb{R}^3 : |x| = 1\}$ is the unit sphere in $\mathbb{R}^3$. For any function $u \in L^2(\partial B_R)$, it admits the Fourier series expansion

$$u(x) := u(R, \hat{x}) = \sum_{n=0}^{\infty} \sum_{m=-n}^{m=n} \hat{u}_n^m(R) Y_n^m(\hat{x}), \quad \hat{u}_n^m = \int_{\mathbb{S}^2} u(R, \hat{x}) \bar{Y}_n^m(\hat{x}) \mathrm{d}\hat{x}.$$

Using the Fourier coefficients, we may define an equivalent $L^2(\partial B_R)$ norm of u as

$$\|u\|_{L^2(\partial B_R)} = \left(\sum_{n=0}^{\infty} \sum_{m=-n}^{n} |\hat{u}_n^m|^2 \right)^{\frac{1}{2}}.$$

The trace space $H^s(\partial B_R)$ is defined by

$$H^s(\partial B_R) = \left\{ u \in L^2(\partial B_R) \ : \ \|u\|_{H^s(\partial B_R)} < \infty \right\},$$

where the norm may be characterized by

$$\|u\|^2_{H^s(\partial B_R)} = \sum_{n=0}^{\infty} \sum_{m=-n}^{m=n} (1 + n(n+1))^s \, |\hat{u}_n^m|^2. \tag{2}$$

Clearly, the dual space of $H^{-s}(\partial B_R)$ is $H^s(\partial B_R)$ with respect to the scalar product in $L^2(\partial B_R)$ defined by

$$\langle u, v \rangle_{\partial B_R} = \int_{\partial B_R} u \bar{v} \mathrm{d}s.$$

In the exterior domain $\mathbb{R}^3 \backslash \overline{B}_R$, the solution of the Helmholtz equation in (1) can be written as

$$u(r, \hat{x}) = \sum_{n=0}^{\infty} \sum_{m=-n}^{n} \hat{u}_n^m \frac{h_n^{(1)}(\kappa r)}{h_n^{(1)}(\kappa R)} Y_n^m(\hat{x}), \quad r > R, \tag{3}$$

where $h_n^{(1)}$ is the spherical Hankel function of the first kind with order n and is defined as (cf. [20])

$$h_n^{(1)}(z) = \sqrt{\frac{\pi}{2z}} H^{(1)}_{n+\frac{1}{2}}(z).$$

Here $H^{(1)}_{n+\frac{1}{2}}(\cdot)$ is the Hankel function of the first kind with order $n + \frac{1}{2}$.

Define the DtN operator $T : H^{\frac{1}{2}}(\partial B_R) \to H^{-\frac{1}{2}}(\partial B_R)$ by

$$(Tu)(R, \hat{x}) = \frac{1}{R} \sum_{n=0}^{\infty} \Theta_n(\kappa R) \sum_{m=-n}^{n} \hat{u}_n^m Y_n^m(\hat{x}), \tag{4}$$

where

$$\Theta_n(z) = z \frac{h_n^{(1)'}(z)}{h_n^{(1)}(z)},$$

which satisfies (cf. [15, 20]):

$$\Re \Theta_n(z) \leq -\frac{1}{2}, \quad \Im \Theta_n(z) > 0, \quad \Theta_n(z) \sim n, \quad n \to \infty. \tag{5}$$

The DtN operator has the following properties. The proof is similar to that of [23, Lemma 1.2] and is omitted here for brevity.

Lemma 2.1. *The DtN operator $T : H^{\frac{1}{2}}(\partial B_R) \to H^{-\frac{1}{2}}(\partial B_R)$ is continuous, i.e.,*

$$\|Tu\|_{H^{-\frac{1}{2}}(\partial B_R)} \lesssim \|u\|_{H^{\frac{1}{2}}(\partial B_R)}.$$

Moreover, it satisfies

$$-\Re \langle Tu, u \rangle \gtrsim \|u\|^2_{L^2(\partial B_R)}, \quad \Im \langle Tu, u \rangle \geq 0.$$

Here $a \lesssim b$ or $a \gtrsim b$ stands for $a \leq Cb$ or $a \geq Cb$, where C is a positive constant whose specific value is not required and may be different in the context.

It follows from (3)–(4) that we have the transparent boundary condition

$$\partial_r u = Tu \quad \text{on } \partial B_R. \tag{6}$$

The weak formulation of (1) is to find $u \in H^1(\Omega)$ such that

$$a(u, v) = \langle g, v \rangle_{\partial D} \quad \forall \, v \in H^1(\Omega), \tag{7}$$

where the sesquilinear form $a: H^1(\Omega) \times H^1(\Omega) \to \mathbb{C}$ is defined by

$$a(u,v) = \int_\Omega \nabla u \cdot \nabla \bar{v} \mathrm{d}x - \kappa^2 \int_\Omega u\bar{v}\mathrm{d}x - \langle Tu, v\rangle_{\partial B_R}$$

and the linear functional

$$\langle g, v\rangle_{\partial D} = \int_{\partial D} g\bar{v}\mathrm{d}s.$$

Theorem 2.2. *The variational problem (7) has at most one solution.*

Proof. It suffices to show that $u = 0$ if $g = 0$. By (7), we have

$$\int_\Omega (|\nabla u|^2 - \kappa^2|u|^2)\mathrm{d}x - \langle Tu, u\rangle_{\partial B_R} = 0.$$

Taking the imaginary part of the above equation yields

$$\Im\langle Tu, u\rangle_{\partial B_R} = R\sum_{n=0}^{\infty}\sum_{m=-n}^{m} \Im\Theta_n(\kappa R)|\hat{u}_n^m|^2 = 0,$$

which gives that $\hat{u}_n^m = 0$ by (5). Thus we have from (3) and (6) that $u = 0$ and $\partial_r u = 0$ on ∂B_R. We conclude from the Holmgren uniqueness theorem and the unique continuation [21] that $u = 0$ on Ω. □

The following result concerns the well-posedness and stability of the variational problem (7). The proof is almost the same as that of [23, Theorem 2.2] and is omitted here for brevity.

Theorem 2.3. *The variational problem (7) admits a unique weak solution u in $H^1(\Omega)$. Furthermore, there is a positive constant C depending on κ and R such that*

$$\|u\|_{H^1(\Omega)} \le C\|g\|_{L^2(\partial D)}.$$

By the general theory in Babuska and Aziz [1], there exists a constant $\gamma > 0$ depending on κ and R such that the following inf-sup condition holds:

$$\sup_{0\neq v\in H^1(\Omega)} \frac{|a(u,v)|}{\|v\|_{H^1(\Omega)}} \ge \gamma\|u\|_{H^1(\Omega)} \quad \forall\, u \in H^1(\Omega).$$

3. **Finite element approximation.** In this section, we introduce the finite element approximation of (7) and present the a posteriori error estimate, which plays an important role in the adaptive finite element method.

Let $\mathcal{M}_h$ be a regular tetrahedral mesh of the domain Ω, where h represents the maximum diameter of all the elements in $\mathcal{M}_h$. In order to avoid using the isoparametric finite element space and discussing the approximation error of the boundaries ∂D and ∂B_R, we assume for simplicity that ∂D and ∂B_R are polyhedral. Thus any face $F \in \mathcal{M}_h$ is a subset of $\partial\Omega$ if it has three boundary vertices.

Let $V_h \subset H^1(\Omega)$ be a conforming finite element space, i.e.,

$$V_h := \{v_h \in C(\overline{\Omega}) : v_h|_K \in P_m(K) \quad \forall\, K \in \mathcal{M}_h\},$$

where m is a positive integer and $P_m(K)$ denotes the set of all polynomials of degree no more than m. The finite element approximation to (7) is to seek $u_h \in V_h$ satisfying

$$a(u_h, v_h) = \langle g, v_h\rangle_{\partial D} \quad \forall\, v_h \in V_h.$$

The above variational problem involves the DtN operator T defined by an infinite series in (4). Practically, it is necessary to truncate the infinite series by taking

finitely many terms of the expansion in order to apply the finite element method. Given a positive integer N, we define the truncated DtN operator

$$(T_N u)(R,\hat{x}) = \frac{1}{R}\sum_{n=0}^{N}\Theta_n(\kappa R)\sum_{m=-n}^{m=n}\hat{u}_n^m Y_n^m(\hat{x}).$$

Using the truncated DtN operator T_N, we have the truncated finite element approximation to the problem (7): Find $u_h^N \in V_h$ such that

$$a_N(u_h^N, v_h) = \langle g, v_h^N\rangle_{\partial D} \quad \forall\, v_h \in V_h, \tag{8}$$

where the sesquilinear form $a_N : V_h \times V_h \to \mathbb{C}$ is defined by

$$a_N(u,v) = \int_\Omega \nabla u\cdot\nabla\bar{v}\mathrm{d}x - \kappa^2\int_\Omega u\bar{v}\mathrm{d}x - \langle T_N u, v\rangle_{\partial B_R}. \tag{9}$$

By the argument of Schatz [30], the discrete inf-sup condition of the sesquilinear form a_N may be established for sufficiently large N and sufficiently small h. It follows from the general theory in [1] that the truncated variational problem (8) admits a unique solution. In this work, our goal is to obtain the a posteriori error estimate and develop the associated adaptive algorithm. Thus we assume that the discrete problem (8) has a unique solution $u_h^N \in V_h$.

4. **A posteriori error analysis.** First, we collect some relevant results from [25] on the Hankel functions. Let $j_n(t)$ and $y_n(t)$ be the spherical Bessel functions of the first and second kind with order n, respectively. The spherical Hankel functions are

$$h_n^{(j)}(t) = j_n(t) \pm \mathrm{i}y_n(t), \quad j = 1, 2.$$

For fixed t, the spherical Bessel functions admit the asymptotic expressions (cf. [25, Theorem 2.31])

$$j_n(t) \sim \frac{t^n}{(2n+1)!!}, \quad y_n(t) \sim -\frac{(2n-1)!!}{t^{n+1}}, \quad n \to \infty,$$

which give that

$$h_n^{(j)}(t) \sim (-1)^j\mathrm{i}\frac{(2n-1)!!}{t^{n+1}}, \quad n \to \infty. \tag{10}$$

For any $K \in \mathcal{M}_h$, let $\mathcal{B}_F$ represent the set of all the faces of K. Denote by h_K and h_F the sizes of element K and face F, respectively. For any interior face F which is the common part of elements K_1 and K_2, we define the jump residual across F as

$$J_F = -(\nabla u_h^N|_{K_1}\cdot\nu_1 + \nabla u_h^N|_{K_2}\cdot\nu_2),$$

where ν_j is the unit normal vector to the boundary of $K_j, j = 1, 2$. For any boundary face $F \in \partial B_R$, we define the jump residual

$$J_F = 2(Tu_h^N + \nabla u_h^N\cdot\nu),$$

where ν is the unit outward normal on ∂B_R. For any boundary face $F \in \partial D$, we define the jump residual

$$J_F = 2(\nabla u_h^N\cdot\nu + g),$$

where ν is the unit outward normal on ∂D pointing toward Ω. For any $K \in \mathcal{M}_h$, denote by η_K the local error estimator, which is defined by

$$\eta_K = h_K\|(\Delta+\kappa^2)u_h^N\|_{L^2(K)} + \Big(\frac{1}{2}\sum_{F\in\partial K} h_F\|J_F\|^2_{L^2(F)}\Big)^{\frac{1}{2}}.$$

We now state the main result, which plays an important role for the numerical experiments.

Theorem 4.1. *Let u and u_h^N be the solutions of (7) and (8), respectively. There exists a positive integer N_0 independent of h such that the following a posteriori error estimate holds for $N > N_0$:*

$$\|u - u_h^N\|_{H^1(\Omega)} \lesssim \left(\sum_{K \in \mathcal{M}_h} \eta_K^2 \right)^{\frac{1}{2}} + \left(\frac{R'}{R} \right)^N \|g\|_{L^2(\partial D)}.$$

It can be seen from Theorem 4.1 that the a posteriori error consists of two parts: the first part comes from the finite element discretization error and the second part accounts for the truncation error of the DtN operator, which decays exponentially with respect to N since $R' < R$. We point out that the constant in the estimate may depend on κ, R and R', but does not depend on the truncation parameter of the DtN operator N or the mesh size of the triangulation h.

In the rest part of this section, we prove the a posteriori error estimator in Theorem 4.1 by using a duality argument.

Denote the error $\xi := u - u_h^N$. Introduce a dual problem to the original scattering problem: Find $w \in H^1(\Omega)$ such that

$$a(v, w) = (v, \xi) \quad \forall\, v \in H^1(\Omega). \tag{11}$$

It is easy to verify that w satisfies the following boundary value problem:

$$\begin{cases} \Delta w + \kappa^2 w = -\xi & \text{in } \mathbb{R}^3 \setminus \overline{D}, \\ \partial_\nu w = 0 & \text{on } \partial D, \\ \partial_r w - T^* w = 0 & \text{on } \partial B_R, \end{cases} \tag{12}$$

where the adjoint operator T^* is defined by

$$(T^* u)(R, \hat{x}) = \frac{1}{R} \sum_{n=0}^{\infty} \overline{\Theta}_n(\kappa R) \sum_{m=-n}^{m=n} \hat{u}_n^m Y_n^m(\hat{x}).$$

We may follow the same proof as that for the original scattering problem (1) and show that the dual problem (12) has a unique weak solution $w \in H^1(\Omega)$, which satisfies

$$\|w\|_{H^1(\Omega)} \lesssim \|\xi\|_{L^2(\Omega)}.$$

The following lemma gives the error representation formulas and is the basis for the a posteriori error analysis.

Lemma 4.2. *Let u, u_h^N and w be the solutions of the problems (7), (8) and (11), respectively. The following identities hold:*

$$\|\xi\|_{H^1(\Omega)}^2 = \Re\left(a(\xi, \xi) + \langle (T - T_N)\xi, \xi \rangle_{\partial B_R}\right) + \Re\langle T_N \xi, \xi \rangle_{\partial B_R} \tag{13}$$

$$+(\kappa^2 + 1)\|\xi\|_{L^2(\Omega)}^2, \tag{14}$$

$$\|\xi\|_{L^2(\Omega)}^2 = a(\xi, w) + \langle (T - T_N)\xi, w \rangle_{\partial B_R} - \langle (T - T_N)\xi, w \rangle_{\partial B_R}, \tag{15}$$

$$a(\xi, \psi) + \langle (T - T_N)\xi, \psi \rangle_{\partial B_R} = \langle g, \psi - \psi_h \rangle_{\partial D} - a_N(u_h^N, \psi - \psi_h)$$

$$+\langle (T - T_N)u, \psi \rangle_{\partial B_R} \quad \forall\, \psi \in H^1(\Omega), \psi_h \in V_h. \tag{16}$$

Proof. The equality (14) follows directly from the definition of the sesquilinear form a in (7). The identity (15) can be easily deduced by taking $v = \xi$ in (11). It remains to prove (16). It follows from (7) and (8) that

$$\begin{aligned} a(\xi,\psi) &= a(u-u_h^N,\psi-\psi_h)+a(u-u_h^N,\psi_h) \\ &= \langle g,\psi-\psi_h\rangle_{\partial D}-a(u_h^N,\psi-\psi_h)+a(u-u_h^N,\psi_h) \\ &= \langle g,\psi-\psi_h\rangle_{\partial D}-a_N(u_h^N,\psi-\psi_h) \\ &\quad +a_N(u_h^N,\psi-\psi_h)-a(u_h^N,\psi-\psi_h)+a(u,\psi_h)-a(u_h^N,\psi_h). \end{aligned}$$

Since $a(u,\psi_h) = \langle g,\psi_h\rangle_{\partial D} = a_N(u_h^N,\psi_h)$, we have

$$\begin{aligned} a(\xi,\psi) &= \langle g,\psi-\psi_h\rangle_{\partial D}-a_N(u_h^N,\psi-\psi_h)+a_N(u_h^N,\psi)-a(u_h^N,\psi) \\ &= \langle g,\psi-\psi_h\rangle_{\partial D}-a_N(u_h^N,\psi-\psi_h)+\langle (T-T_N)u_h^N,\psi\rangle_{\partial B_R} \\ &= \langle g,\psi-\psi_h\rangle_{\partial D}-a_N(u_h^N,\psi-\psi_h)-\langle (T-T_N)\xi,\psi\rangle_{\partial B_R} \\ &\quad +\langle (T-T_N)u,\psi\rangle_{\partial B_R}, \end{aligned}$$

which implies (16) and completes the proof. □

It is necessary to estimate (16) and the last term in (15) in order to prove Theorem 4.1. We begin with a standard trace regularity result. The proof is straightforward and is omitted here for brevity.

Lemma 4.3. *For any $u \in H^1(\Omega)$, the following estimates hold:*

$$\|u\|_{H^{\frac{1}{2}}(\partial B_R)} \lesssim \|u\|_{H^1(\Omega)}, \quad \|u\|_{H^{\frac{1}{2}}(\partial B_{R'})} \lesssim \|u\|_{H^1(\Omega)}.$$

Lemma 4.4. *Let u be the solution to (7). Then the following estimate holds:*

$$|\hat{u}_n^m(R)| \lesssim \Big(\frac{R'}{R}\Big)^n |\hat{u}_n^m(R')|.$$

Proof. It is known that the solution of the scattering problem (1) admits the series expansion

$$u(r,\hat{x}) = \sum_{n=0}^{\infty}\sum_{m=-n}^{n}\frac{h_n^{(1)}(\kappa r)}{h_n^{(1)}(\kappa R')}\hat{u}_n^m(R')Y_n^m(\hat{x}), \quad \hat{u}_n^m(R') = \int_{\mathbb{S}^2} u(R',\hat{x})Y_n^m(\hat{x})\mathrm{d}\hat{x} \tag{17}$$

for all $r > R'$. Evaluating (17) at $r = R$ yields

$$u(R,\hat{x}) = \sum_{n=0}^{\infty}\sum_{m=-n}^{n}\frac{h_n^{(1)}(\kappa R)}{h_n^{(1)}(\kappa R')}\hat{u}_n^m(R')Y_n^m(\hat{x}),$$

which implies

$$\hat{u}_n^m(R) = \frac{h_n^{(1)}(kR)}{h_n^{(1)}(kR')}\hat{u}_n^m(R').$$

Using the asymptotic expression in (10), we obtain

$$|\hat{u}_n^m(R)| = \left|\frac{h_n^{(1)}(kR)}{h_n^{(1)}(kR')}\right||\hat{u}_n^m(R')| \lesssim \Big(\frac{R'}{R}\Big)^n |\hat{u}_n^m(R')|,$$

which completes the proof. □

Lemma 4.5. *For any $\psi \in H^1(\Omega)$, the following estimate holds:*

$$|a(\xi,\psi)+\langle (T-T_N)\xi,\psi\rangle_{\partial B_R}| \lesssim \left(\Big(\sum_{K\in\mathcal{M}_h}\eta_K^2\Big)^{\frac{1}{2}}+\Big(\frac{R'}{R}\Big)^N\|g\|_{L^2(\partial D)}\right)\|\psi\|_{H^1(\Omega)}.$$

Proof. Define

$$\begin{aligned} J_1 &= \langle g,\psi-\psi_h\rangle_{\partial D}-a_N(u_h^N,\psi-\psi_h),\\ J_2 &= \langle (T-T_N)u,\psi\rangle_{\partial B_R}, \end{aligned}$$

where $\psi_h\in V_h$. It follows from (16) that

$$a(\xi,\psi)+\langle (T-T_N)\xi,\psi\rangle_{\partial B_R}=J_1+J_2.$$

Using (9) and the integration by parts, we obtain

$$J_1=\sum_{K\in\mathcal{M}_h}\left(\int_K(\Delta u_h^N+\kappa^2u_h^N)(\bar\psi-\bar\psi_h)\mathrm{d}x+\sum_{F\in\partial K}\frac{1}{2}\int_F J_F(\bar\psi-\bar\psi_h)\mathrm{d}s\right).$$

Now we take $\psi_h=\Pi_h\psi\in V_h$, where Π_h is the Scott–Zhang interpolation operator and has the approximation properties

$$\|v-\Pi_hv\|_{L^2(K)}\lesssim h_K\|\nabla v\|_{L^2(\tilde K)},\quad \|v-\Pi_hv\|_{L^2(F)}\lesssim h_F^{\frac{1}{2}}\|\nabla v\|_{L^2(\tilde K_F)},$$

Here $\tilde K$ and $\tilde K_F$ are the union of all the elements in $\mathcal{M}_h$, which have nonempty intersection with element K and the face F, respectively.

By the Cauchy–Schwarz inequality, we have

$$\begin{aligned} |J_1| &\lesssim \sum_{K\in\mathcal{M}_h}\Big(h_K\|(\Delta+\kappa^2)u_h^N\|_{L^2(K)}\|\nabla\psi\|_{L^2(\tilde K)}\\ &\qquad\qquad +\sum_{F\in\partial K}\frac{1}{2}h_F^{\frac{1}{2}}\|J_F\|_{L^2(F)}\|\psi\|_{H^1(\tilde K_F)}\Big)\\ &\lesssim \sum_{K\in\mathcal{M}_h}\left[h_K\|(\Delta+\kappa^2)u_h^N\|_{L^2(K)}+\Big(\sum_{F\in\partial K}\frac{1}{2}h_F\|J_F\|_{L^2(F)}^2\Big)^{\frac{1}{2}}\right]\|\psi\|_{H^1(\Omega)}\\ &\lesssim \Big(\sum_{K\in\mathcal{M}_h}\eta_K^2\Big)^2\|\psi\|_{H^1(\Omega)}. \end{aligned}$$

It follows from the definitions of T, T_N and Lemma 4.4 that

$$\begin{aligned} |J_2| &= |\langle (T-T_N)u,\psi\rangle_{\partial B_R}|=\Big|R\sum_{n>N}\sum_{|m|\le n}\Theta_n(\kappa R)\hat u_n^m(R)\bar{\hat\psi}_n^m(R)\Big|\\ &\lesssim \sum_{n>N}\sum_{|m|\le n}|\Theta_n(\kappa R)||\hat u_n^m(R)||\bar{\hat\psi}_n^m(R)|\\ &\lesssim \sum_{n>N}\sum_{|m|\le n}|\Theta_n(\kappa R)|\Big|\Big(\frac{R'}{R}\Big)^N\hat u_n^m(R')\Big||\bar{\hat\psi}_{nm}(R)|\\ &\lesssim \Big(\frac{R'}{R}\Big)^N\sum_{n>N}\sum_{|m|\le n}|\Theta_n(\kappa R)||\hat u_n^m(R')||\bar{\hat\psi}_n^m(R)|. \end{aligned}$$

Using (5), the Cauchy–Schwarz inequality, and Lemma 4.3 yields

$$\begin{aligned}
|J_2| &\lesssim \Big(\frac{R'}{R}\Big)^N \sum_{n>N}\sum_{|m|\le n} |\Theta_n(\kappa R)||\hat{u}_n^m(R')||\bar{\hat{\psi}}_n^m(R)| \\
&\lesssim \Big(\frac{R'}{R}\Big)^N \sum_{n>N}(1+n(n+1))^{\frac12}\sum_{|m|\le n} |\hat{u}_n^m(R')||\bar{\hat{\psi}}_n^m(R)| \\
&\le \Big(\frac{R'}{R}\Big)^N \sum_{n>N}(1+n(n+1))^{\frac12}\Big(\sum_{|m|\le n} |\hat{u}_n^m(R')|^2\Big)^{\frac12}\Big(\sum_{|m|\le n} |\bar{\hat{\psi}}_n^m(R)|^2\Big)^{\frac12} \\
&\le \Big(\frac{R'}{R}\Big)^N \Big(\sum_{n>N}(1+n(n+1))^{\frac12}\sum_{|m|\le n} |\hat{u}_n^m(R')|^2\Big)^{\frac12} \\
&\qquad\qquad \Big(\sum_{n>N}(1+n(n+1))^{\frac12}\sum_{|m|\le n} |\bar{\hat{\psi}}_n^m(R)|^2\Big)^{\frac12} \\
&\lesssim \Big(\frac{R'}{R}\Big)^N \|u\|_{H^{\frac12}(\partial B_{R'})}\|\psi\|_{H^{\frac12}(\partial B_R)} \\
&\lesssim \Big(\frac{R'}{R}\Big)^N \|u\|_{H^1(\Omega)}\|\psi\|_{H^{\frac12}(\partial B_R)}.
\end{aligned}$$

Combining the above estimates gives

$$|J_1|+|J_2| \lesssim \bigg(\Big(\sum_{K\in\mathcal{M}_h}\eta_K^2\Big)^{\frac12} + \Big(\frac{R'}{R}\Big)^N \|g\|_{L^2(\partial D)}\bigg)\|\psi\|_{H^1(\Omega)},$$

which completes the proof. □

Lemma 4.6. *Let w be the solution to the dual problem (11). Then the following estimate holds:*

$$|\langle (T-T_N)\xi, w\rangle_{\partial B_R}| \lesssim N^{-2}\|\xi\|^2_{H^1(\Omega)}.$$

Proof. It follows from (5), Lemma 4.3 and the Cauchy–Schwarz inequality that we have

$$\begin{aligned}
|\langle (T-T_N)\xi, w\rangle_{\partial B_R}| &\lesssim \sum_{n>N}\sum_{|m|\le n} |\Theta_n(\kappa R)||\hat{\xi}_n^m(R)||\hat{w}_n^m(R)| \\
&\lesssim \sum_{n>N}\sum_{|m|\le n} |n||\hat{\xi}_n^m(R)||\hat{w}_n^m(R)| \\
&= \sum_{n>N}((1+n^2)^{\frac12}n^3)^{-\frac12}\sum_{|m|\le n}(1+n^2)^{\frac14}n^{\frac52}|\hat{\xi}_n^m(R)||\hat{w}_n^m(R)| \\
&\le N^{-2}\sum_{n>N}\sum_{|m|\le n}(1+n^2)^{\frac14}n^{\frac52}|\hat{\xi}_n^m(R)||\hat{w}_n^m(R)| \\
&\le N^{-2}\Big(\sum_{n>N}\sum_{|m|\le n}(1+n(n+1))^{\frac12}|\hat{\xi}_n^m(R)|^2\Big)^{\frac12}\Big(\sum_{n>N}\sum_{|m|\le n} n^5|\hat{w}_n^m(R)|^2\Big)^{\frac12} \\
&= N^{-2}\|\xi\|_{H^{\frac12}(\partial B_R)}\Big(\sum_{n>N}\sum_{|m|\le n} n^5|\hat{w}_n^m(R)|^2\Big)^{\frac12} \\
&\lesssim N^{-2}\|\xi\|_{H^1(\Omega)}\Big(\sum_{n>N}\sum_{|m|\le n} n^5|\hat{w}_n^m(R)|^2\Big)^{\frac12}.
\end{aligned}$$

To estimate $\hat{w}_n^m(R)$, we consider the dual problem (12) in the annulus $B_R \setminus B_{R'}$:

$$\begin{cases} \Delta w + \kappa^2 w = -\xi & \text{in } B_R \setminus \overline{B}_{R'}, \\ w = w(R', \hat{x}) & \text{on } \partial R', \\ \partial_r w - T^* w = 0 & \text{on } \partial B_R, \end{cases}$$

which reduces to the second order equation for the coefficients $\hat{w}_n^m$ in the Fourier domain

$$\begin{cases} \frac{\mathrm{d}^2 \hat{w}_n^m(r)}{\mathrm{d}r^2} + \frac{2}{r}\frac{\mathrm{d}\hat{w}_n^m(r)}{\mathrm{d}r} + \big(\kappa^2 - \frac{n(n+1)}{r^2}\big)\hat{w}_n^m(r) = -\hat{\xi}_n^m(r), & R' < r < R, \\ \frac{\mathrm{d}\hat{w}_n^m(R)}{\mathrm{d}r} - \frac{1}{R}\overline{\Theta}_n(\kappa R)\hat{w}_n^m(R) = 0, & r = R, \\ \hat{w}_n^m(R') = \hat{w}_n^m(R'), & r = R'. \end{cases}$$

By the method of the variation of parameters, we obtain the solution of the above equation

$$\begin{aligned} \hat{w}_n^m(r) = S_n(r)\hat{w}_n^m(R') + \frac{\mathrm{i}\kappa}{2}\int_{R'}^{r} t^2 W_n(r,t)\hat{\xi}_n^m(t)\mathrm{d}t \\ + \frac{\mathrm{i}\kappa}{2}\int_{R'}^{R} t^2 S_n(t) W_n(R', r)\hat{\xi}_n^m(t)\mathrm{d}t, \end{aligned} \tag{18}$$

where

$$S_n(r) = \frac{h_n^{(2)}(\kappa r)}{h_n^{(2)}(\kappa R')}, \quad W_n(r,t) = \det\begin{bmatrix} h_n^{(1)}(\kappa r) & h_n^{(2)}(\kappa r) \\ h_n^{(1)}(\kappa t) & h_n^{(2)}(\kappa t) \end{bmatrix}.$$

Taking $r = R$ in (18), we get

$$\hat{w}_n^m(R) = S_n(R)\hat{w}_n^m(R') + \frac{\mathrm{i}\kappa}{2}\int_{R'}^{R} t^2 S_n(R) W_n(R', t)\hat{\xi}_n^m(t)\mathrm{d}t.$$

Using the asymptotic expression (10) yields

$$S_n(R) \sim \Big(\frac{R'}{R}\Big)^n, \quad n \to \infty$$

and

$$\begin{aligned} W_n(R', t) &= 2\mathrm{i} j_n(\kappa R') y_n(\kappa R')\Big(\frac{j_n(\kappa t)}{j_n(\kappa R')} - \frac{y_n(\kappa t)}{y_n(\kappa R')}\Big) \\ &\sim -\frac{2\mathrm{i}}{(2n+1)\kappa R'}\Big(\Big(\frac{t}{R'}\Big)^n - \Big(\frac{R'}{t}\Big)^{n+1}\Big), \quad n \to \infty. \end{aligned}$$

Hence

$$|S_n(R)| \lesssim \Big(\frac{R'}{R}\Big)^n, \quad |W_n(R', t)| \lesssim n^{-1}\Big(\frac{t}{R'}\Big)^n.$$

Combining the above estimates, we obtain

$$\begin{aligned} |\hat{w}_n^m(R)| &\le |S_n(R)||\hat{w}_n^m(R')| + \frac{\kappa}{2}\int_{R'}^{R} t^2 |S_n(R)||W_n(R', t)||\hat{\xi}_n^m(t)|\mathrm{d}t, \\ &\lesssim \Big(\frac{R'}{R}\Big)^n |\hat{w}_n^m(R')| + n^{-1}\Big(\frac{R'}{R}\Big)^n \|\hat{\xi}_n^m(t)\|_{L^\infty([R', R])}\int_{R'}^{R} t^2\Big(\frac{t}{R'}\Big)^n \mathrm{d}t \\ &\lesssim \Big(\frac{R'}{R}\Big)^n |\hat{w}_n^m(R')| + n^{-2}\|\hat{\xi}_n^m(t)\|_{L^\infty([R', R])}, \end{aligned}$$

which gives

$$\begin{aligned}
&\sum_{n>N}\sum_{|m|\le n} n^5|\hat{w}_n^m(R)|^2\\
\lesssim\ &\sum_{n>N}\sum_{|m|\le n} n^5\bigg(\Big(\frac{R'}{R}\Big)^n|\hat{w}_n^m(R')|+n^{-2}\|\hat{\xi}_n^m(t)\|_{L^\infty([R',R])}\bigg)^2\\
\lesssim\ &\sum_{n>N}\sum_{|m|\le n} n^5\bigg(\Big(\frac{R'}{R}\Big)^{2n}|\hat{w}_n^m(R')|^2+n^{-4}\|\hat{\xi}_n^m(t)\|^2_{L^\infty([R',R])}\bigg)\\
:=\ & I_1+I_2.
\end{aligned}$$

Here

$$\begin{aligned}
I_1&=\sum_{n>N}\sum_{|m|\le n} n^5\Big(\frac{R'}{R}\Big)^{2n}|\hat{w}_n^m(R')|^2,\\
I_2&=\sum_{n>N}\sum_{|m|\le n} n\|\hat{\xi}_n^m(t)\|^2_{L^\infty([R',R])}.
\end{aligned}$$

A simple calculation yields

$$\begin{aligned}
I_1\ &\lesssim\ \max_{n>N} n^4\Big(\frac{R'}{R}\Big)^{2n}\sum_{n>N}\sum_{|m|\le n} n\ |\hat{w}_n^m(R')|^2\lesssim\sum_{n>N}\sum_{|m|\le n} n\ |\hat{w}_n^m(R')|^2\\
&\lesssim\ \sum_{n>N}(1+n^2)^{\frac12}\sum_{|m|\le n}|\hat{w}_n^m(R')|^2\le\|w\|^2_{H^{\frac12}(\partial B_{R'})}\lesssim\|\xi\|^2_{H^1(\Omega)}.
\end{aligned}$$

By [22, Lemma 5], we have

$$\|\hat{\xi}_n^m(t)\|^2_{L^\infty([R',R])}\le\Big(\frac{2}{\delta}+n\Big)\|\hat{\xi}_n^m(t)\|^2_{L^2([R',R])}+n^{-1}\|\hat{\xi}_n^{m'}(t)\|^2_{L^2([R',R])},$$

where $\delta=R-R'$. Following a similar proof of Lemma 4.2 yields

$$\begin{aligned}
\|\xi\|^2_{H^1(B_R\setminus\overline{B}_R)}&\ge\sum_{n=0}^{\infty}\sum_{|m|\le n}\int_{R'}^{R}\Big[(r^2+n(n+1))|\xi_n^m(r)|^2+r^2|\xi_n^{m'}(r)|^2\Big]\,\mathrm{d}r\\
&\ge\sum_{n=0}^{\infty}\sum_{|m|\le n}\int_{R'}^{R}\Big[(R'^2+n(n+1))|\xi_n^m(r)|^2+R'^2|\xi_n^{m'}(r)|^2\Big]\,\mathrm{d}r,
\end{aligned}$$

which gives

$$I_2=\sum_{n>N}\sum_{|m|\le n} n\|\hat{\xi}_{nm}(t)\|^2_{L^\infty([R',R])}\lesssim\|\xi\|^2_{H^1(\Omega)}.$$

Therefore, we obtain

$$\sum_{n>N}\sum_{|m|\le n} n^5|\hat{w}_n^m(R)|^2\lesssim\|\xi\|^2_{H^1(\Omega)},$$

which completes the proof. □

Now we prove the main theorem.

Proof. We conclude from (4)–(5) that

$$\Re\langle T_N\xi,\xi\rangle_{\partial B_R}=R\sum_{n=0}^{N}\sum_{|m|\le n}\Re(\Theta(\kappa R))|\hat{\xi}_n^m|^2\le 0.$$

It follows from (14) and Lemma 4.4 that there exist two positive constants C_1 and C_2 independent of h and N satisfying

$$\|\xi\|^2_{H^1(\Omega)} \le C_1\bigg(\Big(\sum_{K\in\mathcal{M}_h}\eta_K^2\Big)^{\frac{1}{2}} + \Big(\frac{R'}{R}\Big)^N\|g\|_{L^2(\partial D)}\bigg)\|\xi\|_{H^1(\Omega)} + C_2\|\xi\|_{L^2(\Omega)}.$$

Using (15) and Lemmas 4.4–4.5, we obtain

$$\|\xi\|^2_{L^2(\Omega)} \le C_3\bigg(\Big(\sum_{K\in\mathcal{M}_h}\eta_K^2\Big)^{\frac{1}{2}} + \Big(\frac{R'}{R}\Big)^N\|g\|_{L^2(\partial D)}\bigg)\|\xi\|_{L^2(\Omega)} + C_4N^{-2}\|\xi\|_{H^1(\Omega)},$$

where C_3 and C_4 are positive constants independent of h and N. Combining the above estimates yields

$$\|\xi\|^2_{H^1(\Omega)} \le C_5\bigg(\Big(\sum_{K\in\mathcal{M}_h}\eta_K^2\Big)^{\frac{1}{2}} + \Big(\frac{R'}{R}\Big)^N\|g\|_{L^2(\partial D)}\bigg)\|\xi\|_{H^1(\Omega)} + C_6N^{-2}\|\xi\|_{H^1(\Omega)},$$

where C_5 and C_6 are positive constants independent of h and N. We may choose a sufficiently large integer N_0 such that $C_6N_0^{-2} < 1/2$, which completes the proof by taking $N > N_0$. □

5. **Numerical experiments.** In this section, we discuss the implementation of the adaptive finite element algorithm with the truncated DtN boundary condition and present two numerical examples to demonstrate the competitive performance of the proposed method. There are two components which need to be designed carefully in order to efficiently implement the h-adaptive method. The first one is an effective management mechanism of the mesh grids. The other one is an effective indicator for the adaptivity. The a posteriori error estimate from Theorem 4.1 is used to generate the indicator in our algorithm.

5.1. **The hierarchy geometry tree.** In our algorithm, we use the hierarchy geometry tree (HGT) or the hierarchical grids to manage the data structure of the mesh grids [4]. The structure of the grids is described hierarchically. For example, the element such as a point for 0-dimension, an edge for 1-dimension, a triangle for 2-dimension, a tetrahedron for 3-dimension is called a geometry. If a triangle is one of the faces of a tetrahedron, then it belongs to this tetrahedron. Similarly, if an edge is one of the edges of a triangle, then it belongs to this triangle. Hence all geometries in the tetrahedrons have belonging-to relationship.

A tetrahedron T_0 can be uniformly divided into eight small sub-tetrahedrons $\{T_{0,0}, T_{0,1}\cdots T_{0,7}\}$. In this refinement operation, every face of the tetrahedron is divided into four smaller triangles. This procedure can be managed by the octree data structure which is given by Figure 1, which shows that the sub-tetrahedrons $T_{0,0}$ and $T_{0,6}$ are further divided into eight smaller sub-tetrahedrons. In the octree, we name T_0 as the root node and those nodes without further subdivision like $T_{0,1}$ and $T_{0,0,0}$ as the leaf nodes. Obviously, a set of root nodes $\{T_i\}, i = 0, 1, \cdots$ can form a three-dimensional initial mesh for a domain Ω and a set of all the leaf nodes of the HGTs also form a mesh.

By using the HGT, the refinement and even the coarsening of a mesh can be done efficiently. However, it may cause the hanging points in the direct neighbors of the refined tetrahedrons. In order to remove these hanging points, two kinds of geometries may be introduced: twin-tetrahedron and four-tetrahedron. For the twin-tetrahedron geometry as shown in Figure 2 (left), it has five degrees of freedom (DoF) and consists of two standard tetrahedrons. To conform the finite

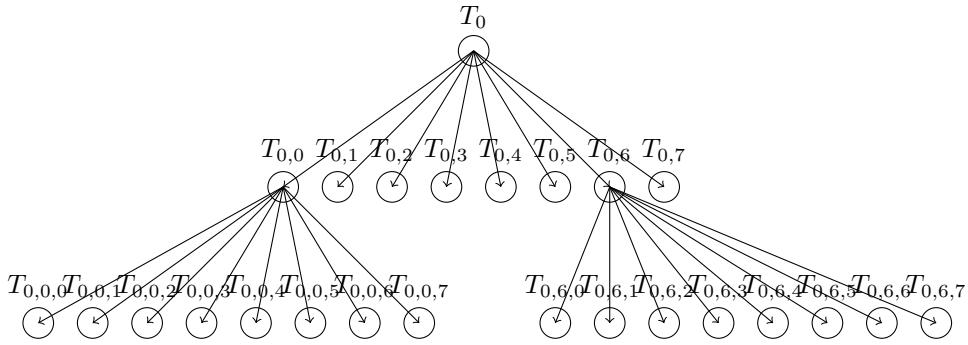

FIGURE 1. A schematic of octree data structure.

element space, the following strategy is used to construct the basis function in twin-tetrahedron geometry. For each basis function, the value is 1 at the corresponding interpolation point and the value is 0 at the other interpolation points. For the common point of the two sub-tetrahedrons in the twin-tetrahedron like A, D and E, the support of the basis function is the whole twin-tetrahedron. For the points B and C, the support of their corresponding basis function is only the tetrahedron ABED and the tetrahedron AECD, respectively. For the four-tetrahedron as shown in Figure 2 (right), the similar strategy is used. With the twin-tetrahedron geometry and the four-tetrahedron geometry, the local refinement can be implemented easily.

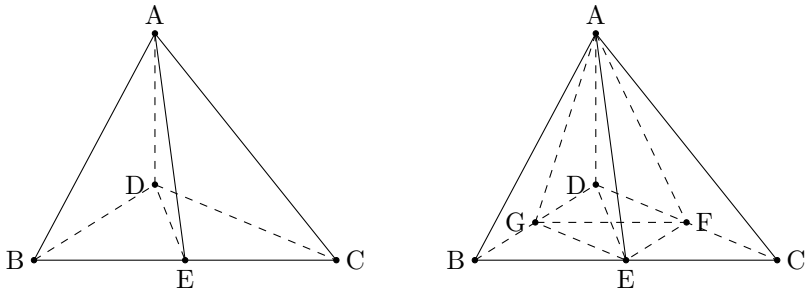

FIGURE 2. Two geometries to avoid hanging points. (left) Twin-tetrahedron geometry. (right) Four-tetrahedron geometry.

In practice, we use a polyhedral surface to approximate ∂D and ∂B_R. Since the TBC operator is represented by the spherical harmonic functions whose accuracy depends on how good the approximation is. Obviously, a rough approximation could not satisfy the computational requirement. Based on the element geometry introduced above, we present a method to deal with the surface refinement. Suppose that the domain Ω has a curved boundary and the initial mesh is given by a rough polygon. The traditional surface refinement is performed by taking the midpoint of each side of the tetrahedron. Hence the shape of the boundary cannot be well approximated. To resolve this issue, a very simple method is adopted. When the boundary elements of the mesh need to be refined, we redefine the midpoint through projecting vertically to the desired curved boundary, as shown in Figure 3.

Thanks to the HGTs, it does not spend much time at all to find these boundary elements. This method works efficiently in two-dimensions. But in three-dimensions, it may cause the neighbors to become non-standard twin-tetrahedron geometry or four-tetrahedrons geometry. To handle this problem, these special tetrahedrons, whose neighbors do not need refinement, should not redefine the midpoint. So the marked boundary tetrahedron will not be refined until the neighboring boundary tetrahedrons are marked in order to keep the mesh structure.

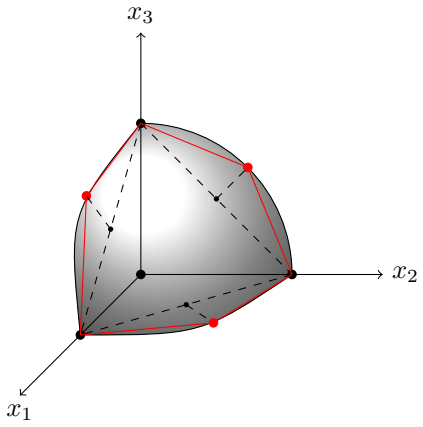

FIGURE 3. Mesh refinement on the surface (red points are redefined midpoints on the boundary).

5.2. **The adaptive algorithm.** The numerical simulations are implemented with a C++ library: Adaptive Finite Element Package (AFEPack). The initial mesh is generated by GMSH[16]. The resulting sparse linear systems are solved by the solver called Eigen. The simulations are implemented on a HP workstation and are accelerated by using OpenMP. The a posteriori error estimate from Theorem 4.1 is adopted to generate the indicators in our algorithm.

The error consists of two parts: the finite element discretization error ε_h and the DtN operator truncation error ε_N which depends on N. Specifically,

$$\varepsilon_h = \Big(\sum_{K\in\mathcal{M}_h} \eta_K^2 \Big)^{\frac{1}{2}} = \eta_{\mathcal{M}_h}, \quad \varepsilon_N = \Big(\frac{R'}{R}\Big)^N \|g\|_{L^2(\partial D)}. \tag{19}$$

In the implementation, we can choose R', R, and N based on (19) such that finite element discretization error is not contaminated by the truncation error, i.e., ε_N is required to be very small compared with ε_h, for example, $\varepsilon_N \le 10^{-8}$. For simplicity, in the following numerical experiments, R' is chosen such that the scatterer lies exactly in the circle $B_{R'}$ and N is taken to be the smallest positive integer satisfying $\varepsilon_N \le 10^{-8}$. Table 1 shows the adaptive finite element algorithm with the DtN boundary condition for solving the scattering problem.

5.3. **Numerical examples.** We present two numerical examples to illustrate the performance of the proposed method. In the implementation, the wavenumber is $\kappa = \pi$, which accounts for the wavelength $\lambda = 2\pi/\kappa = 2$.

Example 1. Let the obstacle $D = B_{0.5}$ be the ball with a radius of 0.5 and $\Omega = B_1 \setminus \overline{B}_{0.5}$ be the computational domain. The boundary condition g is chosen

TABLE 1. The adaptive FEM-DtN algorithm.

1	Given a tolerance $\varepsilon > 0$;
2	Choose R, R' and N such that $\varepsilon_N < 10^{-8}$;
3	Construct an initial tetrahedral partition $\mathcal{M}_h$ over Ω and compute error estimators;
4	While $\eta_K > \varepsilon$, do
5	mark K, refine $\mathcal{M}_h$, and obtain a new mesh $\hat{\mathcal{M}}_h$.
6	solve the discrete problem on the $\hat{\mathcal{M}}_h$.
7	compute the corresponding error estimators;
8	End while.

such that the exact solution is

$$u(x) = \frac{e^{\mathrm{i}\kappa r}}{r}, \quad r = |x|.$$

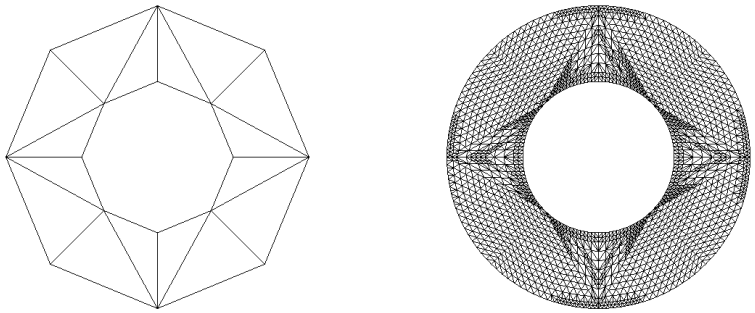

FIGURE 4. Example 1: (left) initial mesh on the x_1x_2-plane. (right) adaptive mesh on the x_1x_2-plane.

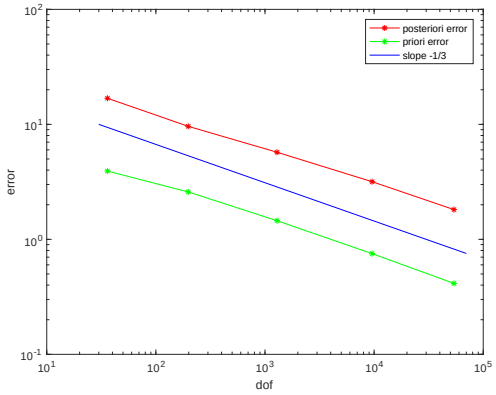

FIGURE 5. Example 1: quasi-optimality of the a priori and a posteriori error estimates.

The initial mesh and an adaptive mesh is shown in Figure 4. Figure 5 displays the curves of $\log e_h$ and $\log \varepsilon_h$ versus $\log \mathrm{DoF}_h$ for our adaptive DtN method, where $e_h = \|\nabla(u - u_h^N)\|_{L^2(\Omega)}$ is the a priori error, ε_h is the a posteriori error given in (19), and Dof_h denotes the degree of freedom or the number of nodal points of the mesh $\mathcal{M}_h$ in the domain Ω. It indicates that the meshes and associated numerical complexity are quasi-optimal, i.e., $\|\nabla(u - u_h^N)\|_{L^2(\Omega)} = \mathcal{O}(\mathrm{DoF}_h^{-\frac{1}{3}})$ holds asymptotically.

Example 2. This example concerns the scattering of the plane wave $u^{\mathrm{inc}} = e^{\mathrm{i}\kappa x_3}$ by a U-shaped obstacle D which is contained in the box $\{x \in \mathbb{R}^3 : -0.25 \leq x_1, x_2, x_3 \leqslant 0.25\}$. There is no analytical solution for this example and the solution contains singularity around the corners of the obstacle. The Neumann boundary condition is set by $g = \partial_\nu u^{\mathrm{inc}}$ on ∂D. We take $R = 1$, $R' = \frac{\sqrt{3}}{4}$ for the adaptive DtN method. Figure 6 shows the cross section of the obstacle and the adaptive mesh of 63898 elements, and the curve of $\log \varepsilon_h$ versus $\log \mathrm{DoF}_h$. It implies that the decay of the a posteriori error estimate is $\mathcal{O}(\mathrm{DoF}_h^{-1/3})$, which is optimal.

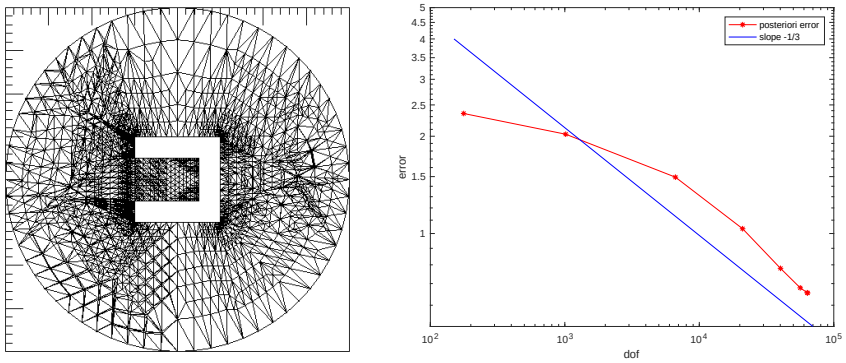

FIGURE 6. Example 2: (left) an adaptively refined mesh with 63898 elements. (right) quasi-optimality of the a posteriori error estimate.

6. **Conclusion.** In this paper, we have presented an adaptive finite element method with the transparent boundary condition for the three-dimensional acoustic obstacle scattering problem. The truncated DtN operator was considered for the discrete problem. A dual argument was developed in order to derive the a posteriori error estimate. The error consists of the finite element approximation error and the DtN operator truncation error which was shown to exponentially decay with respect to the truncation parameter N. Numerical results show that the method is effective to solve the three-dimensional acoustic obstacle scattering problem. Possible future work is to extend the adaptive FEM-DtN method for solving the three-dimensional electromagnetic and elastic obstacle scattering problems, where the wave propagation is governed by the Maxwell equations and the Navier equation, respectively. We hope to report the progress on solving these problems elsewhere in the future.

REFERENCES

[1] I. Babuška and A. Aziz, Survey Lectures on mathematical foundations of the finite element method, in *The Mathematical Foundations of the Finite Element Method with Application to the Partial Differential Equations*, ed. by A. Aziz, Academic Press, New York, 1972, 1–359.

[2] G. Bao, R. Delgadillo, G. Hu, D. Liu and S. Luo, Modeling and computation of nano-optics, *CSIAM Trans. Appl. Math.*.
[3] G. Bao, Y. Gao and P. Li, Time-domain analysis of an acoustic-elastic interaction problem, *Arch. Ration. Mech. Anal.*, **229** (2018), 835–884.
[4] G. Bao, G. Hu and D. Liu, An h-adaptive finite element solver for the calculations of the electronic structures, *J. Comput. Phys.*, **231** (2012), 4967–4979.
[5] G. Bao, P. Li and H. Wu, An adaptive edge element method with perfectly matched absorbing layers for wave scattering by periodic structures, *Math. Comp.*, **79** (2010), 1–34.
[6] G. Bao and H. Wu, Convergence analysis of the perfectly matched layer problems for time-harmonic Maxwell's equations, *SIAM J. Numer. Anal.*, **43** (2005), 2121–2143.
[7] A. Bayliss and E. Turkel, Radiation boundary conditions for wave-like equations, *Comm. Pure Appl. Math.*, **33** (1980), 707–725.
[8] J.-P. Berenger, A perfectly matched layer for the absorption of electromagnetic waves, *J. Comput. Phys.*, **114** (1994), 185–200.
[9] Z. Chen and X. Liu, An adaptive perfectly matched layer technique for time-harmonic scattering problems, *SIAM J. Numer. Anal.*, **43** (2005), 645–671.
[10] Z. Chen and H. Wu, An adaptive finite element method with perfectly matched absorbing layers for the wave scattering by periodic structures, *SIAM J. Numer. Anal.*, **41** (2003), 799–826.
[11] F. Collino and P. Monk, The perfectly matched layer in curvilinear coordinates, *SIAM J. Sci. Comput.*, **19** (1998), 2061–2090.
[12] D. L. Colton and R. Kress, *Integral Equation Methods in Scattering Theory*, John Wiley & Sons, New York, 1983.
[13] D. Colton and R. Kress, *Inverse Acoustic and Electromagnetic Scattering Theory*, Second Edition, Springer, Berlin, New York, 1998.
[14] B. Engquist and A. Majda, Absorbing boundary conditions for the numerical simulation of waves, *Math. Comp.*, **31** (1977), 629–651.
[15] Q. Fang, D. P. Nicholls and J. Shen, A stable, high-order method for three-dimensional, bounded-obstacle, acoustic scattering, *J. Comput. Phys.*, **224** (2007), 1145–1169.
[16] C. Geuzaine and J.-F. Remacle, GMSH: A three-dimensional finite element mesh generator with built-in pre- and post-processing facilities, *Internat. J. Numer. Methods Engrg.*, **79** (2009), 1309–1331.
[17] M. J. Grote and J. B. Keller, On nonreflecting boundary conditions, *J. Comput. Phys.*, **122** (1995), 231–243.
[18] M. J. Grote and C. Kirsch, Dirichlet-to-Neumann boundary conditions for multiple scattering problems, *J. Comput. Phys.*, **201** (2004), 630–650.
[19] T. Hagstrom, Radiation boundary conditions for the numerical simulation of waves, *Acta Numerica*, **8** (1999), 47–106.
[20] I. Harari and T. J. R. Hughes, Analysis of continuous formulations underlying the computation of time-harmonic acoustics in exterior domains, *Comput. Methods Appl. Mech. Engrg.*, **97** (1992), 103–124.
[21] D. Jerison and C. Kenig, Unique continuation and absence of positive eigenvalues for Schrodinger operators, *Ann. Math.*, **121** (1985), 463–488.
[22] X. Jiang, P. Li, J. Lv and W. Zheng, An adaptive finite element method for the wave scattering with transparent boundary condition, *J. Sci. Comput.*, **72** (2017), 936–956.
[23] X. Jiang, P. Li and W. Zheng, Numerical solution of acoustic scattering by an adaptive DtN finite element method, *Commun. Comput. Phys.*, **13** (2013), 1227–1244.
[24] J. Jin, *The Finite Element Method in Electromagnetics*, Second edition. New York, 2002.
[25] A. Kirsch and F. Hettlich, *The Mathematical Theory of Time-Harmonic Maxwell's Equations*, Springer International Publishing, 2015.
[26] P. Li and X. Yuan, Convergence of an adaptive finite element DtN method for the elastic wave scattering by periodic structures, *Comput. Methods Appl. Mech. Engrg.*, **360** (2020), 112722.
[27] Y. Li, W. Zheng and X. Zhu, A CIP-FEM for high-frequency scattering problem with the truncated DtN boundary condition, *CSIAM Trans. Appl. Math.*, **1** (2020), 530–560.
[28] P. Monk, *Finite Element Methods for Maxwell's Equations*, Oxford University Press, New York, 2003.
[29] J.-C. Nédélec, *Acoustic and Electromagnetic Equations Integral Representations for Harmonic Problems*, Springer-Verlag, New York, 2001.

[30] A. H. Schatz, An observation concerning Ritz–Galerkin methods with indefinite bilinear forms, *Math. Comp.*, **28** (1974), 959–962.
[31] E. Turkel and A. Yefet, Absorbing PML boundary layers for wave-like equations, *Appl. Numer. Math.*, **27** (1998), 533–557.
[32] Z. Wang, G. Bao, J. Li, P. Li and H. Wu, An adaptive finite element method for the diffraction grating problem with transparent boundary condition, *SIAM J. Numer. Anal.*, **53** (2015), 1585–1607,
[33] X. Yuan, G. Bao and P. Li, An adaptive finite element DtN method for the open cavity scattering problems, *CSIAM Trans. Appl. Math.*, **1** (2020), 316–345.

Received July 2020; revised October 2020.

E-mail address: baog@zju.edu.cn
E-mail address: mmzaip@zju.edu.cn
E-mail address: binh@zju.edu.cn
E-mail address: lipeijun@math.purdue.edu